



**SIMPLE, POWERFUL, ACCESSIBLE.  
FULL SPECTRUM FLOW CYTOMETRY**

9+ color assays, together with high throughput or extended warranty, for just \$69.9K

**ACT NOW**



## **Engulfment of Apoptotic Cells by Macrophages: A Role of MicroRNA-21 in the Resolution of Wound Inflammation**

This information is current as of December 11, 2020.

Amitava Das, Kasturi Ganesh, Savita Khanna, Chandan K. Sen and Sashwati Roy

*J Immunol* 2014; 192:1120-1129; Prepublished online 3 January 2014;

doi: 10.4049/jimmunol.1300613

<http://www.jimmunol.org/content/192/3/1120>

**References** This article **cites 66 articles**, 23 of which you can access for free at: <http://www.jimmunol.org/content/192/3/1120.full#ref-list-1>

**Why *The JI*? Submit online.**

- **Rapid Reviews! 30 days\*** from submission to initial decision
- **No Triage!** Every submission reviewed by practicing scientists
- **Fast Publication!** 4 weeks from acceptance to publication

*\*average*

**Subscription** Information about subscribing to *The Journal of Immunology* is online at: <http://jimmunol.org/subscription>

**Permissions** Submit copyright permission requests at: <http://www.aai.org/About/Publications/JI/copyright.html>

**Email Alerts** Receive free email-alerts when new articles cite this article. Sign up at: <http://jimmunol.org/alerts>

*The Journal of Immunology* is published twice each month by The American Association of Immunologists, Inc., 1451 Rockville Pike, Suite 650, Rockville, MD 20852  
Copyright © 2014 by The American Association of Immunologists, Inc. All rights reserved.  
Print ISSN: 0022-1767 Online ISSN: 1550-6606.



# Engulfment of Apoptotic Cells by Macrophages: A Role of MicroRNA-21 in the Resolution of Wound Inflammation

Amitava Das, Kasturi Ganesh, Savita Khanna, Chandan K. Sen, and Sashwati Roy

At an injury site, efficient clearance of apoptotic cells by wound macrophages or efferocytosis is a prerequisite for the timely resolution of inflammation. Emerging evidence indicates that microRNA-21 (miR-21) may regulate the inflammatory response. In this work, we sought to elucidate the significance of miR-21 in the regulation of efferocytosis-mediated suppression of innate immune response, a key process implicated in resolving inflammation following injury. An increased expression of inducible miR-21 was noted in post-efferocytotic peripheral blood monocyte-derived macrophages. Such induction of miR-21 was associated with silencing of its target genes PTEN and PDCD4. Successful efferocytosis of apoptotic cells by monocyte-derived macrophages resulted in the suppression of LPS-induced NF- $\kappa$ B activation and TNF- $\alpha$  expression. Interestingly, bolstering of miR-21 levels alone, using miR mimic, resulted in significant suppression of LPS-induced TNF- $\alpha$  expression and NF- $\kappa$ B activation. We report that efferocytosis-induced miR-21, by silencing PTEN and GSK3 $\beta$ , tempers the LPS-induced inflammatory response. Macrophage efferocytosis is known to trigger the release of anti-inflammatory cytokine IL-10. This study demonstrates that following successful efferocytosis, miR-21 induction in macrophages silences PDCD4, favoring c-Jun–AP-1 activity, which in turn results in elevated production of anti-inflammatory IL-10. In summary, this work provides direct evidence implicating miRNA in the process of turning on an anti-inflammatory phenotype in the post-efferocytotic macrophage. Elevated macrophage miR-21 promotes efferocytosis and silences target genes PTEN and PDCD4, which in turn accounts for a net anti-inflammatory phenotype. Findings of this study highlight the significance of miRs in the resolution of wound inflammation. *The Journal of Immunology*, 2014, 192: 1120–1129.

**E**fferocytosis, a term coined by deCathelineau and Henson (1) and Gardai et al. (2), refers to phagocytosis of apoptotic cells (3). Efferocytosis is the final fate of apoptotic cells at an injury site. Successful efferocytosis drives timely resolution of inflammation (4–7). Defective clearance of apoptotic cells has been linked to autoimmunity and persistent inflammatory diseases (8). In contrast to uptake of pathogens or FcR-mediated phagocytosis, the engulfment of apoptotic cells does not lead to proinflammatory cytokine production by macrophages (9). Thus, efferocytosis is noninflammatory and nonimmunogenic (10).

MicroRNAs (miRs), 19–22 nucleotides long, are noncoding RNAs found in all eukaryotic cells (11). These noncoding small RNAs regulate ~30% of the human genome, primarily through translational repression (12). miRs were linked with immune responses in a study in which miR expression profiling was performed in a monocytic cell line treated with LPS, a ligand for TLR4 (13). The expression of miR-146a, miR-155, and miR-132 was induced in response to LPS stimulation (13, 14). Although the role of miRs in inflammatory responses associated with cancer has been extensively studied (15–18), information on their role in regulating efferocytosis-mediated immune

suppression and resolution of inflammation is scanty. It has been commonly noted that inflammatory stimuli induce miR-21 (19, 20). A single primary transcript containing miR-21 (pri-miR-21) is transcribed from an evolutionarily conserved promoter that resides in an intron of an overlapping coding gene, TMEM49 (21). PTEN and the tumor suppressor PDCD4 have been identified as one of the first validated direct targets that are translationally silenced by miR-21 (22, 23). Recent evidences indicate that miR-21 may serve as a rheostat to control the inflammatory response (24). In one of the first works that noted the anti-inflammatory properties of miR-21 in macrophages, it was reported that miR-21 silences the proinflammatory IL-12 (25). In the lungs, miR-21 inhibited TLR 2 agonist-induced lung inflammation in mice (26). miR-21 is inducible by resolvin D1, an endogenous lipid mediator generated during the resolution phase of acute inflammation. Thus, miR-21 has been proposed to play a role in resolving acute inflammation (27). Beyond its direct effects on macrophages, miR-21 acts on a number of biological targets validated in a variety of cell types, pointing to an overall anti-inflammatory role (24). As an anti-inflammatory agent, miR-21 silences PTEN as well as PDCD4 (24, 28). In this work, we sought to elucidate the significance of miR-21 in the regulation of efferocytosis-mediated suppression of innate immune response, a key process implicated in resolving inflammation following injury.

## Materials and Methods

### *Peripheral blood monocyte-derived macrophages*

Human PBMCs were isolated from fresh blood leukocyte source packs (American Red Cross, Columbus, OH) by density gradient centrifugation using a Ficoll-Hypaque density gradient (GE Healthcare, formerly Amersham Biosciences, Piscataway, NJ). Positive selection for monocytes was performed using CD14 Ab conjugated to magnetic beads (Miltenyi Biotec, Auburn, CA). Purity of these preparations of monocytes was > 90%, as determined by FACS analyses using CD14 Abs. Differentiation of these cells to monocyte-derived macrophages (MDMs) was performed as described (29).

Department of Surgery, Davis Heart and Lung Research Institute, Center for Regenerative Medicine and Cell Based Therapies and Comprehensive Wound Center, The Ohio State University Wexner Medical Center, Columbus, OH 43210

Received for publication March 7, 2013. Accepted for publication November 7, 2013.

This work was supported by National Institute of Diabetes and Digestive and Kidney Diseases Grant R01 DK076566 (to S.R.) and National Institute of General Medical Sciences Grants GM069589, GM 077185, and NR013898 (to C.K.S.).

Address correspondence and reprint requests to Dr. Sashwati Roy, 473 West 12th Avenue, 511 DHLRI, The Ohio State University Medical Center, Columbus, OH 43210. E-mail address: sashwati.roy@osumc.edu

Abbreviations used in this article: bpV, bisperoxovanadium; GSK3, glycogen synthase kinase 3; IKK- $\beta$ , I $\kappa$ B kinase; MDM, monocyte-derived macrophage; miR, microRNA; si, small interfering.

Copyright © 2014 by The American Association of Immunologists, Inc. 0022-1767/14/\$16.00

### Apoptotic cell clearance (efferocytosis) assay

MDMs were seeded in six-well plates. Apoptosis in Jurkat cells was induced by treating the cells with anti-Fas Ab (human, activating), clone CH11 (250 ng/ml; Millipore, Temecula, CA). Apoptotic Jurkat cells (Clone E6-1; American Type Culture Collection, Manassas, VA) were added to MDM cultures at a ratio of (1:10) macrophage:Jurkat cell. The coculture and efferocytosis assay was performed as described previously (4). Following completion of efferocytosis assay, LPS was added to the culture media, as specified in figure legends.

### ELISA

For measurement of IL-10 and TNF- $\alpha$  produced by macrophages, cells were seeded in 6-well or 12-well plates and cultured in RPMI 1640 medium containing 10% heat-inactivated bovine serum under standard culture conditions. After a specified duration, the culture media were collected and IL-10 and TNF- $\alpha$  levels were measured using commercially available ELISA kits (R&D Systems, Minneapolis, MN) according to the manufacturer's instructions (4, 29).

### Reverse transcription and quantitative RT-PCR

Total RNA was extracted using the mirVana RNA Isolation Kit (Ambion, Austin, TX), according to the manufacturer's instructions. mRNA was quantified by real-time or quantitative PCR assay using the dsDNA binding dye SYBR Green I, as described previously (29–31). For determination of miR expression, specific TaqMan assays for miRs and the TaqMan Micro-RNA Reverse Transcription Kit were used, followed by real-time PCR using the Universal PCR Master Mix (Applied Biosystems, Foster City, CA) (22, 32, 33).

### miRIDIAN miR mimic/inhibitor and small interfering RNA delivery

DharmaFECT 1 Transfection Reagent (Dharmacon RNA Technologies, Lafayette, CO) was used to transfect cells with miRIDIAN mimic-miR-21 or inhibitor miR-21 (Dharmacon RNA Technologies, Lafayette, CO) for 72 h per the manufacturer's instructions. miRIDIAN miR mimic/inhibitor negative controls (Dharmacon RNA Technologies) were used for control

transfections. Small interfering (si) RNA transfections were performed as described (29, 31). In brief, DharmaFECT 1 was used to transfect cells with a 100-nM siRNA pool of PTEN, PDCD4, or c-Jun (Dharmacon RNA technologies) for 72 h. For control, a siControl nontargeting siRNA pool (mixture of four siRNAs, designed to have four or more mismatches with the gene) was used. With this approach, the transfection efficiency was ~70%.

### Western blot

Western blot was performed using primary Ab against PDCD4, PTEN, phospho-p65, phospho-I $\kappa$ B- $\alpha$ , I $\kappa$ B- $\alpha$ , phospho-I $\kappa$ B kinase (IKK)- $\beta$ , IKK- $\beta$ , phospho-c-Jun (Cell Signaling), and c-Jun (Santa Cruz Biotechnology), as described previously (31, 34, 35). Membranes were probed with anti-GAPDH or  $\beta$ -actin Ab to control for sample loading.

### Adenoviral delivery of PTEN, NF- $\kappa$ B luciferase reporter, and AP-1 luciferase reporter

Primary human macrophages were infected with adenovirus encoding for PTEN (Applied Biological Materials, Vancouver, BC, Canada), NF- $\kappa$ B promoter luciferase reporter or AP-1 luciferase reporter gene (Vector Biolabs, Philadelphia, PA), as described previously (22, 36). After 72-h infection, cells were harvested for protein, NF- $\kappa$ B reporter, or AP-1 reporter luciferase assay.

### DNA binding of NF- $\kappa$ B

Nuclear protein extracts of cells were prepared using the Nuclear Extraction Kit (Active Motif, Carlsbad, CA) according to the manufacturer's instructions. Binding of the NF- $\kappa$ B family of proteins to their consensus sites was determined using an ELISA-based Trans-AM NF- $\kappa$ B Kit (Active Motif).

### miR-target 3'-UTR luciferase reporter assay

miRIDIAN mimic-miR-21 was transfected to HEK293 cells, followed by transfection with pGL3-PTEN-3'-UTR plasmid or lenti luc-PDCD4-3'UTR (SABiosciences, Frederick, MD). Luciferase assays were performed using the reporter assay system (Promega, Madison, WI) as described (32, 33).

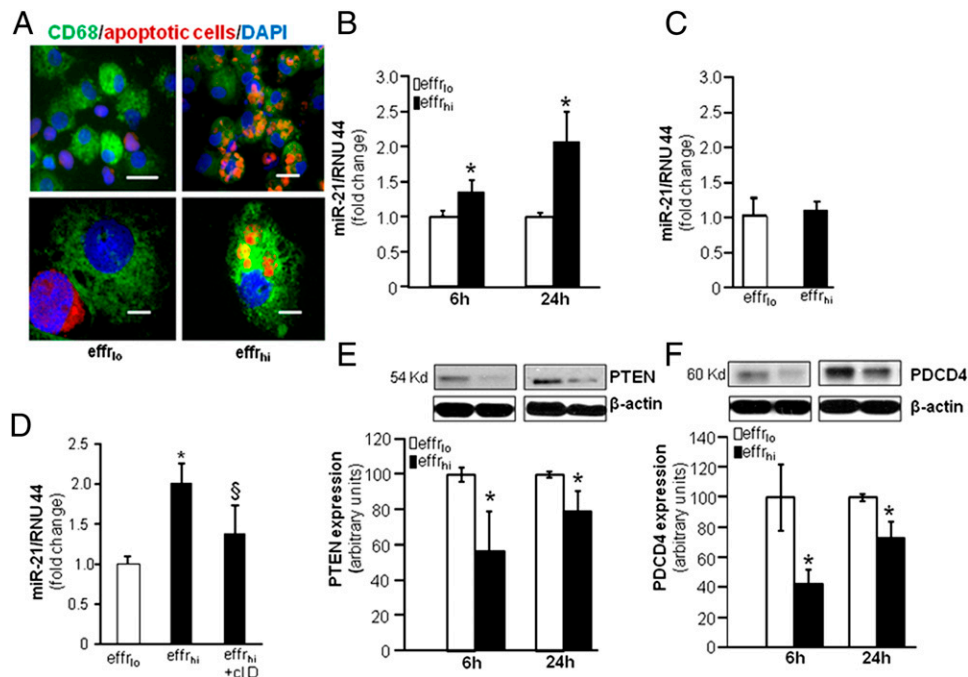


**FIGURE 1.** Increased expression of miR-21 and silencing of target proteins PTEN and PDCD4 in MDMs following engulfment of apoptotic cells (efferocytosis). For efferocytosis assay, blood MDMs were cocultured with apoptotic or viable Jurkat T cells. Nonefferocytosed Jurkat cells were removed by washing with saline. (A) Representative images of MDM (green), CD68 (apoptotic or viable Jurkat T cells) (red), CMTMR cell tracker) cells. Cells were counterstained with DAPI (nuclear, blue). (B) MiR-21 expression in effr<sub>0</sub> or effr<sub>hi</sub> groups following 6 or 24 h of LPS (1  $\mu$ g/ml) treatment. Data are mean  $\pm$  SD ( $n = 4$ ); \* $p < 0.05$  compared with the effr<sub>0</sub> group. (C) MiR-21 expression in effr<sub>0</sub> or effr<sub>hi</sub> groups post efferocytosis. Data are mean  $\pm$  SD ( $n = 6$ ). (D) miR-21 expression in cells pretreated with cytochalasin D (c1D; 1  $\mu$ g/ml, 1 h) followed by efferocytosis and LPS treatment. miR-21 expression was measured 24 h post LPS treatment. Data are mean  $\pm$  SD ( $n = 4$ ); \* $p < 0.05$  compared with macrophages cultured with effr<sub>0</sub>, <sup>ns</sup> $p < 0.05$  compared with macrophages cultured with the effr<sub>hi</sub> group. (E and F) Expression of miR-21 target proteins, (E) PTEN and (F) PDCD4, in effr<sub>0</sub> or effr<sub>hi</sub> groups following 6 or 24 h of LPS (1  $\mu$ g/ml) treatment, measured using Western blot. Quantification of PTEN or PDCD4 levels was performed using densitometry. Data were normalized to  $\beta$ -actin. Data are mean  $\pm$  SD ( $n = 3$ ). \* $p < 0.05$  compared with macrophages cultured with the effr<sub>0</sub> group.

### AP-1 reporter assay

For AP-1 transcriptional activation assay, HEK293 TLR4/IL-1R1/MD-2 cells were provided by Dr. Mikhail Gavrilin at The Ohio State University (37). Cells were transfected with 500 ng AP-1 plasmid (Stratagene California, La Jolla, CA) using Lipofectamine LTX/Plus Reagent (Invitrogen, Grand Island, NY) according to the manufacturer's protocol. After 48 h, cells were transfected with control or miR-21 mimic for 72 h. Luciferase activity was determined using the luciferase reporter assay system (Promega).

### Statistics

Data are reported as mean  $\pm$  SD of three to four experiments, as indicated in the respective figure legends. Comparisons among multiple groups were tested using ANOVA. A  $p$  value  $\leq$  0.05 was considered statistically significant.

## Results

### Increased expression of LPS-inducible miR-21 following efferocytosis

We determined whether successful efferocytosis or engulfment of apoptotic cells by macrophages regulates the expression of miR-21. For efferocytosis assay, MDMs were cocultured with apoptotic (effr<sub>hi</sub>) or viable (effr<sub>lo</sub>) Jurkat T cells. Such coculture resulted in successful engulfment of apoptotic Jurkat cells, but not the viable cells (Fig. 1A). The current study addressed efferocytosis associated

with inflammatory settings. Inflammatory response in engulfing MDMs was induced by treating cells with the TLR-4 agonist LPS. Following LPS treatment (6 h or 24 h), the expression of miR-21 was increased in MDMs that engulfed apoptotic cells compared with MDMs that were cocultured with viable cells (Fig. 1B). In the absence of the TLR-4 agonist, miR-21 expression in MDMs cocultured with viable or apoptotic cells remained unaltered (Fig. 1C). To test whether the LPS-induced miR-21 expression response is specific to efferocytosis, the cytoskeleton was disrupted using cytochalasin D. Cytochalasin D is known to block efferocytosis by disrupting actin polymerization (38). Preincubation with cytochalasin D blocked efferocytosis-mediated miR-21 induction (Fig. 1D). Furthermore, miR-21 expression in macrophages remained unaltered in response to phagocytosis of bacteria (not shown). These two lines of evidence support that induction of miR-21 is a response specifically caused by efferocytosis. Finally, induction of miR-21 expression was associated with silencing of its target genes PTEN and PDCD4 (Fig. 1E, 1F).

### Efferocytosis-induced miR-21 suppressed the proinflammatory NF- $\kappa$ B-TNF $\alpha$ pathway

Under proinflammatory conditions such as the presence of pathogenic microbial stimuli, the engulfment of apoptotic cells by macrophage suppressed production of the proinflammatory cytokine

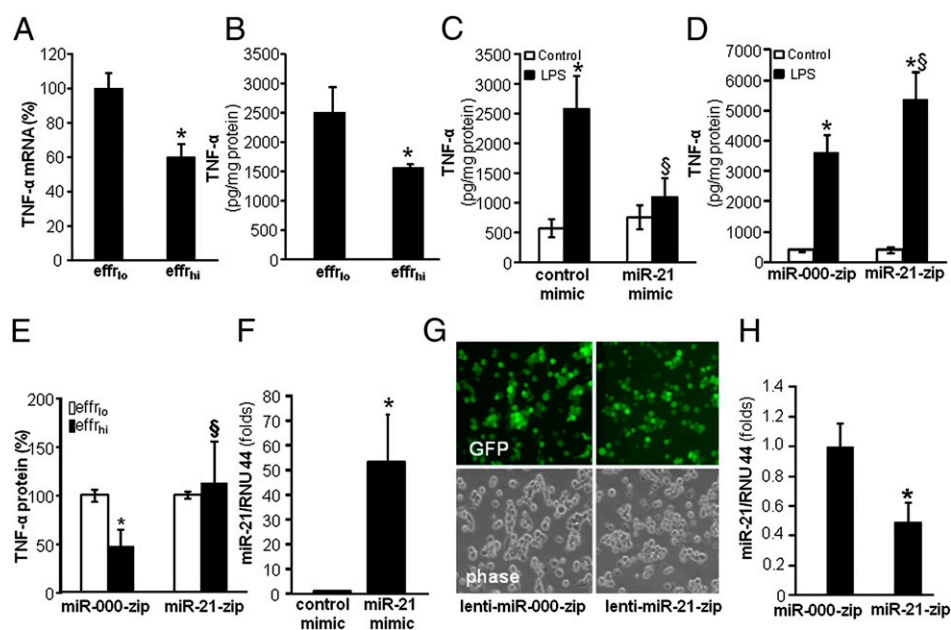


**FIGURE 2.** miR-21 is required for efferocytosis-induced suppression of proinflammatory TNF- $\alpha$  expression. (A and B) For efferocytosis assay, blood MDMs were cocultured with either viable (effr<sub>lo</sub>) or apoptotic (effr<sub>hi</sub>) Jurkat T cells for 1 h. Nonefferocytosed cells were removed by washing with saline. Cells were treated with LPS (1  $\mu$ g/ml) for 6 h (mRNA) or 24 h (protein) post efferocytosis. TNF- $\alpha$  (A) mRNA and (B) protein expression were measured using quantitative PCR and ELISA, respectively. Data are mean  $\pm$  SD ( $n$  = 4); \* $p$  < 0.05 compared with macrophages cultured with the effr<sub>lo</sub> group. (C) MDMs were transfected with miRIDIAN hsa-miR-21 mimic or control mimic to increase miR-21 levels. Cells were activated with LPS (1  $\mu$ g/ml) for 24 h after forced expression of miR-21 in MDMs. The TNF- $\alpha$  protein levels in cells were determined using ELISA. Data are mean  $\pm$  SD ( $n$  = 4); \* $p$  < 0.05 compared with macrophages transfected with control mimic group, § $p$  < 0.05 compared with control mimic LPS-treated group. (D) Stable knockdown of miR-21 in THP-1 monocytic cells was achieved following lentiviral transduction with lenti-miR-000-zip or lenti-miR-21-zip vectors and puromycin selection. The THP-1 cells with stable knockdown of miR-21 were cultured and differentiated to macrophages with PMA (20 ng/ml, 48 h). Cells were activated with LPS (1  $\mu$ g/ml) for 24 h. TNF- $\alpha$  protein released by the cells in culture media was determined using ELISA. Data are mean  $\pm$  SD ( $n$  = 4); \* $p$  < 0.05 compared with macrophages not treated with LPS, § $p$  < 0.05 compared with the miR-000-zip LPS-treated group. (E) Loss of miR-21 in macrophages results in abrogation of efferocytosis-mediated suppression of LPS-induced TNF- $\alpha$  expression. MiR-000-zip or miR-21-zip cells were subjected to efferocytosis, followed by treatment with LPS for 24 h. TNF- $\alpha$  protein levels in cells were determined using ELISA. Data are mean  $\pm$  SD ( $n$  = 4); \* $p$  < 0.05 compared with macrophages cultured with the effr<sub>lo</sub> group, § $p$  < 0.05 compared with miR-000-zip cells. (F) miR-21 expression in miRIDIAN hsa-miR-21 mimic or control mimic transfected cells. Data are mean  $\pm$  SD ( $n$  = 4); \* $p$  < 0.05 compared with macrophages transfected with control mimic. (G) GFP (green) and phase contrast (phase) images of THP-1 cells showing transduction efficiency following lentiviral transduction with lenti-miR-000-zip or lenti-miR-21-zip vectors and puromycin selection showing that > 80% cells were GFP positive. (H) miR-21 expression in miR-000-zip or miR-21-zip cells. Data are mean  $\pm$  SD ( $n$  = 4); \* $p$  < 0.05 compared with miR-000-zip cells.

TNF- $\alpha$  and induced the production of anti-inflammatory cytokine IL-10 (39–41). Successful efferocytosis of apoptotic Jurkat cells by MDMs resulted in suppression of LPS-induced TNF- $\alpha$  levels both at mRNA as well as at protein levels (Fig. 2A, 2B). Of interest, isolated bolstering of miR-21 levels in MDMs using miR mimic (miRIDIAN hsa-miR-21, Fig. 2F) resulted in significant suppression of LPS-induced TNF- $\alpha$  expression (Fig. 2C). Lenti-miR-000-zip or lenti-miR-21-zip vectors and puromycin selection were used to generate THP-1 cells with stable knockdown of miR-21 (Fig. 2G, 2H). Such THP-1 cells with stable knockdown of miR-21 expression were differentiated to macrophages, as described (29). In these cells, LPS-induced TNF- $\alpha$  levels were further potentiated, compared with those of LPS-treated miR-000-zip THP-1 cells (Fig. 2D). Finally, efferocytosis-dependent suppression of LPS-induced TNF- $\alpha$  expression was significantly blocked in cells with stable knockdown of miR-21 levels (Fig. 2E). In summary, these data establish that elevated miR-21 causes efferocytosis-induced suppression of inducible TNF- $\alpha$  expression.

NF- $\kappa$ B is one of the major transcription factors that drive inducible TNF- $\alpha$  expression in macrophages (42). We tested whether efferocytosis may influence LPS-induced NF- $\kappa$ B activation. Both DNA binding activity of NF- $\kappa$ B in nuclear extracts of MDMs and NF- $\kappa$ B transcriptional activation, as measured using NF- $\kappa$ B-

dependent luciferase reporter gene (Ad5NF $\kappa$ B-LUC), were significantly inhibited in MDMs cocultured with apoptotic cells (effr<sub>hi</sub>) compared with that in MDMs cocultured with viable cells (effr<sub>lo</sub>; Fig. 3A, 3B). LPS-induced phosphorylation of I $\kappa$ B as well as of the NF- $\kappa$ B subunit p65 in macrophages plays a critical role in NF- $\kappa$ B transactivation (43). Efferocytosis significantly inhibited LPS-induced p65 phosphorylation (Fig. 3C). Comparable to the effect of efferocytosis, increase or knockdown in miR-21 levels in MDM was inversely related to phosphorylation of p65 and I $\kappa$ B, indicating direct regulation of NF- $\kappa$ B activation by miR-21 in MDMs (Fig 3E–G). Bolstering miR-21 in MDMs by miR mimic delivery did not influence TLR-4 mRNA expression, suggesting that miR-21 acts downstream of TLR-4 (Fig 3D). The delivery of miR-21 mimic to MDM, however, did enhance efferocytosis (Fig. 3H).

*miR-21 target PTEN exacerbated LPS-induced TNF- $\alpha$  expression by potentiating NF- $\kappa$ B activation*

Using miR mimic, knockdown and PTEN-3'-UTR firefly luciferase expression construct, we observed that PTEN is a direct target of miR-21 in MDMs (Fig 4A–C). Overexpression of PTEN in MDMs using adenoviral-PTEN vector (Fig. 5G) resulted in increased LPS-induced TNF- $\alpha$  production (Fig. 5A). Vanadate derivatives such as the bisperoxovanadium (bpV) function as phosphatase

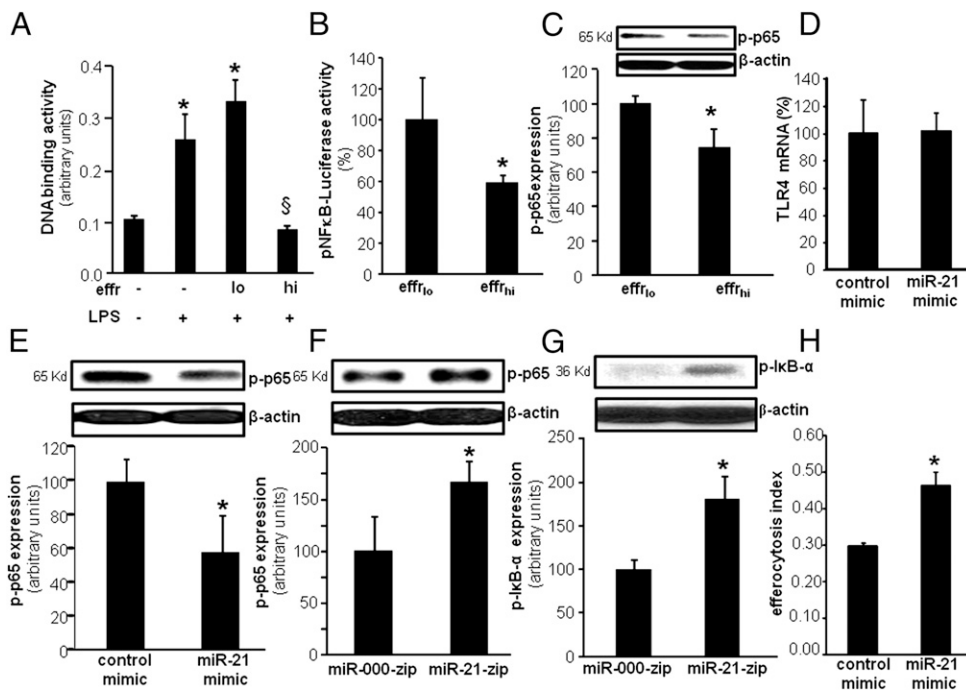


**FIGURE 3.** Efferocytosis-induced miR-21 suppressed the proinflammatory NF- $\kappa$ B-activation. (A–C) For efferocytosis assay, blood MDMs were cocultured with either viable (effr<sub>lo</sub>) or apoptotic (effr<sub>hi</sub>) Jurkat T cells for 1 h. Nonefferocytosed cells were removed by washing with saline. Cells were treated with LPS (1  $\mu$ g/ml) for 6 h post efferocytosis. (A) DNA binding activity of NF- $\kappa$ B in MDMs measured using an ELISA-based (Trans-AM) method. \* $p$  < 0.05 compared with macrophages not stimulated with LPS;  $^{\#}p$  < 0.05 compared with macrophages cultured with the effr<sub>lo</sub> group. (B) NF- $\kappa$ B transcriptional activity in MDMs transiently transfected with NF- $\kappa$ B-dependent luciferase reporter gene (Ad5NF $\kappa$ B-LUC) followed by coculture with either viable (effr<sub>lo</sub>) or apoptotic (effr<sub>hi</sub>) Jurkat T cells for 1 h and LPS treatment (6 h). Luciferase activity was determined. Data are mean  $\pm$  SD ( $n$  = 4). \* $p$  < 0.05 compared with macrophages cultured with the effr<sub>lo</sub> group. (C) Phosphorylation of p65 protein was measured using Western blot in human macrophages following efferocytosis and LPS treatment (1  $\mu$ g/ml). Quantification of phospho-p65 level was performed using densitometry. Data were normalized to  $\beta$ -actin. \* $p$  < 0.05 compared with macrophages cultured with the effr<sub>lo</sub> group. (D) TLR4 mRNA expression in MDMs transfected with miRIDIAN hsa-miR-21 mimic or control mimic. Data are mean  $\pm$  SD ( $n$  = 3). (E) Phosphorylation of NF- $\kappa$ B p65 in MDMs transfected with miRIDIAN hsa-miR-21 mimic or control mimic to increase miR-21 levels. Cells were activated with LPS after forced expression of miR-21 in MDMs. Serine 536 phosphorylation on p65 was determined using Western blot. Quantification of phospho-p65 level was performed using densitometry. Data were normalized to  $\beta$ -actin. Data are mean  $\pm$  SD ( $n$  = 3); \* $p$  < 0.05 compared with control mimic transfected cells. (F) LPS induced phosphorylation of p65 in THP-1 monocytic cells in which stable knockdown of miR-21 was achieved following lentiviral transduction with lenti-miR-000-zip or lenti-miR-21-zip vectors. Data are mean  $\pm$  SD ( $n$  = 3); \* $p$  < 0.05 compared with control miR-000-zip cells. (G) LPS induced phosphorylation of I $\kappa$ B (serine 32) in THP-1 monocytic cells in which stable knockdown of miR-21 was achieved following lentiviral transduction with lenti-miR-000-zip or lenti-miR-21-zip vectors. Data are mean  $\pm$  SD ( $n$  = 3); \* $p$  < 0.05 compared with control miR-000-zip cells. (H) Efferocytosis index of MDMs after delivery of miR-21 mimic. Data are presented as mean  $\pm$  SD ( $n$  = 3); \* $p$  < 0.05 compared with control.

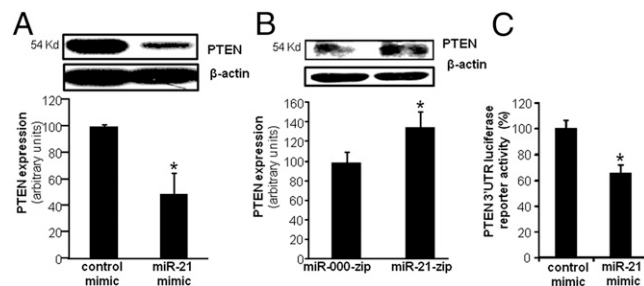


**FIGURE 4.** PTEN is a direct target of miR-21 in human macrophages. **(A)** PTEN expression in MDMs transfected with miRIDIAN hsa-miR-21 mimic or control mimic to increase miR-21 expression. PTEN levels were determined using Western blot. Quantification of PTEN level was performed using densitometry. Data were normalized to  $\beta$ -actin. Data are mean  $\pm$  SD ( $n = 3$ );  $*p < 0.05$  compared with control mimic transfected cells. **(B)** PTEN expression in stably knocked down miR-21 THP-1 monocytic cells. PTEN protein expression was measured using Western blot. Data are mean  $\pm$  SD ( $n = 3$ );  $*p < 0.05$  compared with control miR-000-zip cells. **(C)** To demonstrate that PTEN is a direct target for miR-21, HEK293 cells were transfected with a pGL3-PTEN-3'-UTR firefly luciferase expression construct and cotransfected with pRL-TK Renilla luciferase expression construct along with either miR-21 mimic or control mimic. Data represent mean  $\pm$  SD ( $n = 3$ );  $*p < 0.05$  compared with control transfected cells.

inhibitors in micromolar concentration (44). bpV(phen) specifically inhibits PTEN in nanomolar concentrations (44). Potent inhibition of LPS-induced TNF- $\alpha$  production was noted with MDMs treated with bpV(phen) (100 nM) (Fig. 5B), indicating a supporting role of PTEN in LPS-induced TNF- $\alpha$  production. Furthermore, PTEN inhibition using siPTEN or bpV(phen) blocked inducible TNF- $\alpha$  production under conditions of miR-21 depletion (Fig. 5C, 5D). These data suggest that PTEN plays a critical role in miR-21-mediated regulation of TNF- $\alpha$ . Next, we

determined the effect of PTEN on LPS-induced NF- $\kappa$ B activation. Both LPS-induced NF- $\kappa$ B transactivation using NF- $\kappa$ B-Luc reporter construct and phospho-p65 induction were further potentiated in MDMs in which forced expression of PTEN was achieved using adPTEN. These findings support the idea that high PTEN levels in cells increase LPS-induced NF- $\kappa$ B activation and, therefore, TNF- $\alpha$  expression (Fig. 5E, 5F). Thus, the PTEN silencing effects of miR-21 may account for its anti-inflammatory function.

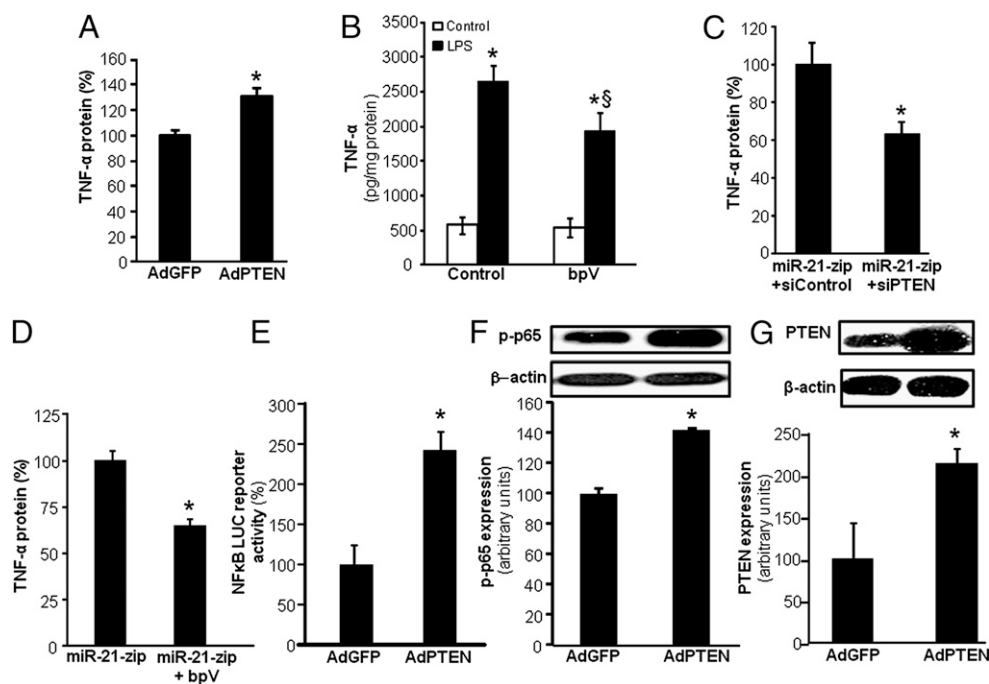


**FIGURE 5.** miR-21 silences LPS-induced NF- $\kappa$ B signaling and TNF- $\alpha$  expression via a PTEN-dependent mechanism. **(A)** TNF- $\alpha$  protein expression was measured in MDMs infected with adenovirus-PTEN vector or adenovirus GFP vectors followed by LPS treatment (1  $\mu$ g/ml) for 24 h. Data are mean  $\pm$  SD ( $n = 4$ );  $*p < 0.05$  compared with macrophages infected with adenovirus GFP vectors. **(B)** TNF- $\alpha$  protein expression was measured in MDMs treated with bpV(phen) (100 nM), a PTEN inhibitor, followed by LPS treatment. Data are mean  $\pm$  SD ( $n = 4$ );  $*p < 0.05$  compared with cells not treated with LPS,  $^{\$}p < 0.05$  compared with control group treated with LPS. **(C and D)** Effect of PTEN knockdown using (C) siPTEN or (D) PTEN inhibitor bpV(phen) on LPS-inducible TNF- $\alpha$  protein expression in THP-1 monocytic cells in which stable knockdown of miR-21 was achieved following lentiviral transduction with lenti-miR-000-zip or lenti-miR-21-zip vectors. TNF- $\alpha$  protein expression was determined in PTEN knockdown cells after LPS (1  $\mu$ g/ml) for 24 h. Data are mean  $\pm$  SD ( $n = 4$ );  $*p < 0.05$  compared with control miR-21-zip cells. **(E)** LPS-inducible NF- $\kappa$ B transcription activity in MDMs transiently transfected with NF- $\kappa$ B-dependent luciferase reporter gene (Ad5NF $\kappa$ B-LUC) followed by infection with adenovirus-PTEN or adenovirus GFP (control) vectors. Luciferase activity was determined. Data are mean  $\pm$  SD ( $n = 4$ ).  $*p < 0.05$  compared with control adenovirus GFP-infected cells. **(F)** Phosphorylation of p65 protein was measured using Western blot in MDMs infected with adenovirus-PTEN or adenovirus GFP vectors followed by LPS treatment (1  $\mu$ g/ml). Data are mean  $\pm$  SD ( $n = 3$ );  $*p < 0.05$  compared with control adenovirus GFP-infected cells. **(G)** PTEN protein expression was measured using Western blot in MDMs infected with adenovirus-PTEN vector or adenovirus GFP vectors. Quantification of PTEN level was performed using densitometry. Data are mean  $\pm$  SD ( $n = 3$ );  $*p < 0.05$  compared with control adenovirus GFP-infected cells.

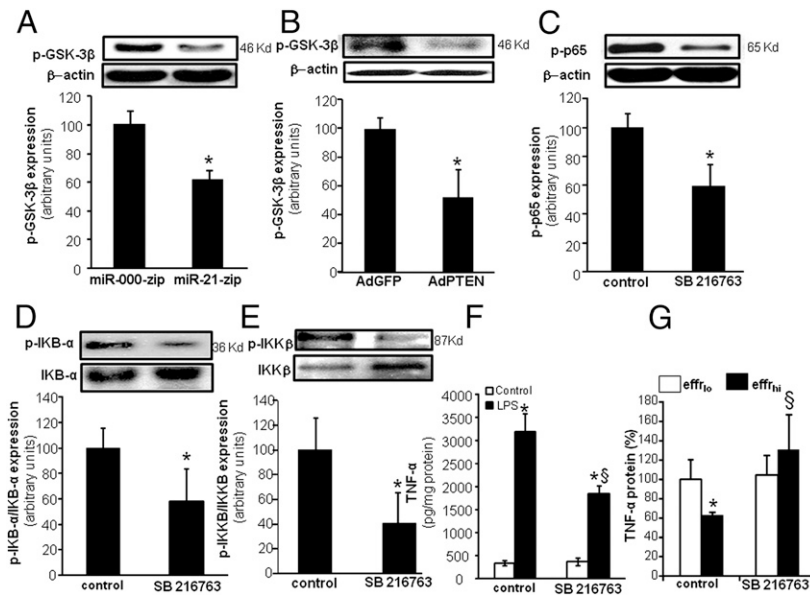


**FIGURE 6.** miR-21 silencing of PTEN inhibited GSK3 $\beta$ , which in turn inhibited inducible NF- $\kappa$ B activation. **(A)** Phosphorylation of GSK3 $\beta$  (serine 9) in THP-1 monocytic cells in which stable knockdown of miR-21 was achieved following lentiviral transduction with lenti-miR-000-zip or lenti-miR-21-zip vectors followed by LPS treatment (1  $\mu$ g/ml). Data are mean  $\pm$  SD ( $n = 3$ ); \* $p < 0.05$  compared with miR-000-zip cells. **(B)** Phosphorylation of GSK3 $\beta$  protein was measured using Western blot in MDMs infected with adenovirus-PTEN or adenovirus GFP vectors followed by LPS treatment. Data are mean  $\pm$  SD ( $n = 3$ ); \* $p < 0.05$  compared with control adenovirus GFP-infected cells. **(C)** Phosphorylation of NF- $\kappa$ B p65 protein was measured using Western blot in MDMs treated with 10  $\mu$ M SB 216763 (GSK3 $\beta$  inhibitor) followed by LPS treatment. Quantification was performed using densitometry. Data are mean  $\pm$  SD ( $n = 3$ ); \* $p < 0.05$  compared with control cells. **(D)** Phosphorylation of I $\kappa$ B- $\alpha$  protein in MDMs treated with 10  $\mu$ M SB 216763, followed by LPS treatment. Data are mean  $\pm$  SD ( $n = 3$ ); \* $p < 0.05$  compared with control cells. **(E)** Phosphorylation of IKK- $\beta$  protein (serine 181) in MDMs treated with 10  $\mu$ M SB 216763, followed by LPS treatment. Data are mean  $\pm$  SD ( $n = 3$ ); \* $p < 0.05$  compared with control cells. **(F)** TNF- $\alpha$  protein expression was measured in MDMs treated with 10  $\mu$ M SB 216763 followed by LPS treatment. Data are mean  $\pm$  SD ( $n = 4$ ); \* $p < 0.05$  compared with non-LPS-treated cells, <sup>§</sup> $p < 0.05$  compared with control group treated with LPS. **(G)** TNF- $\alpha$  protein expression in MDMs pretreated with 10  $\mu$ M SB 216763 followed by efferocytosis and LPS treatment. Data are mean  $\pm$  SD ( $n = 3$ ); \* $p < 0.05$  compared with effro group, <sup>§</sup> $p < 0.05$  compared with group not treated with SB 216763.

#### miR-21 silencing of PTEN inhibited GSK3 $\beta$ implicated in NF- $\kappa$ B activation and inducible TNF- $\alpha$ expression

PTEN blocks the action of PI3K by dephosphorylating the signaling lipid phosphatidylinositol (3,4,5)-triphosphate. Thus, PTEN antagonizes signaling through the PI3K pathway (45). The PI3K/Akt signaling pathway is a major regulator of glycogen synthase kinase 3 (GSK3). GSK3 isoforms are normally constitutively active in a cell, and they are regulated through inhibition (46). GSK3 $\beta$  activity can be downregulated by phosphorylation at the N-terminal region serine 9, which leads to the inhibition of this isoform (46). In general, phosphorylation at serine 9 has been used as a marker for inactive GSK3 $\beta$  (46). Knockdown of miR-21 and overexpression of PTEN both resulted in strong inhibition in the phosphorylation of GSK3 $\beta$ . Thus, lowering of miR-21 levels in human macrophages resulted in increased GSK3 $\beta$  activity via a PTEN-dependent mechanism (Fig. 6A, 6B). Inhibition of GSK3 $\beta$  activity using a specific inhibitor, SB 216763, lowered the abundance of phospho-p65 as well as lowered phospho-I $\kappa$ B and phospho-IKK- $\beta$  abundance (Fig. 6C–E). Thus, LPS-induced NF- $\kappa$ B activation is dependent on GSK3 $\beta$  activity. Pharmacological inhibition of GSK3 $\beta$  activity resulted in significant inhibition of LPS-induced TNF- $\alpha$  expression (Fig. 6F). These findings support a role for GSK3 $\beta$  in miR-21–PTEN-mediated regulation of LPS-induced NF- $\kappa$ B activation and TNF- $\alpha$  expression. Finally, pharmacological inhibition of GSK3 $\beta$  negated the ability of efferocytosis to blunt inducible TNF- $\alpha$  expression, supporting a key role of GSK3 $\beta$  in the efferocytosis-dependent resolution of the inflammation pathway (Fig. 6G).

#### Successful efferocytosis potentiates inducible IL-10 expression via a miR-21-dependent mechanism

IL-10 is an anti-inflammatory cytokine (39–41). After successful efferocytosis, human MDMs showed enhanced IL-10 expression (Fig. 7A, 7B). MDMs transfected with miRIDIAN hsa-miR-21 mimic to increase miR-21 levels also showed increased IL-10 protein levels compared with MDMs transfected with control mimic (Fig. 7C). These observations support the idea that an elevated cellular miR-21 level is sufficient to potentiate inducible IL-10 in macrophages. Efferocytosis-dependent induction of IL-10 was attenuated under conditions of miR-21 inhibition, demonstrating a role for miR-21 (Fig. 7D). IL-10 is known to inhibit the production of LPS-induced proinflammatory cytokines by macrophages (47). We observe that adding IL-10 to LPS-induced MDMs dose dependently inhibited inducible TNF- $\alpha$  release from cells, supporting potent anti-inflammatory activity of IL-10 (Fig. 7E).

#### miR-21 potentiated inducible IL-10 expression via a PDCD4-c-Jun-AP-1 pathway

To determine the mechanisms of miR-21-mediated potentiation of inducible IL-10 expression, MDMs were transfected with miRIDIAN hsa-miR-21 mimic to increase cellular miR-21 abundance. PDCD4 is a confirmed target of miR-21 in macrophages (48). Our results support that finding and show that elevation of miR-21 levels inhibited PDCD4 expression in MDMs (Fig. 8A). Elevated cellular miR-21 also inhibited luciferase reporter activity in cells transfected with PDCD4 3'UTR-luciferase reporter construct (Fig. 8B), establishing PDCD4 as a direct target of miR-21. To test

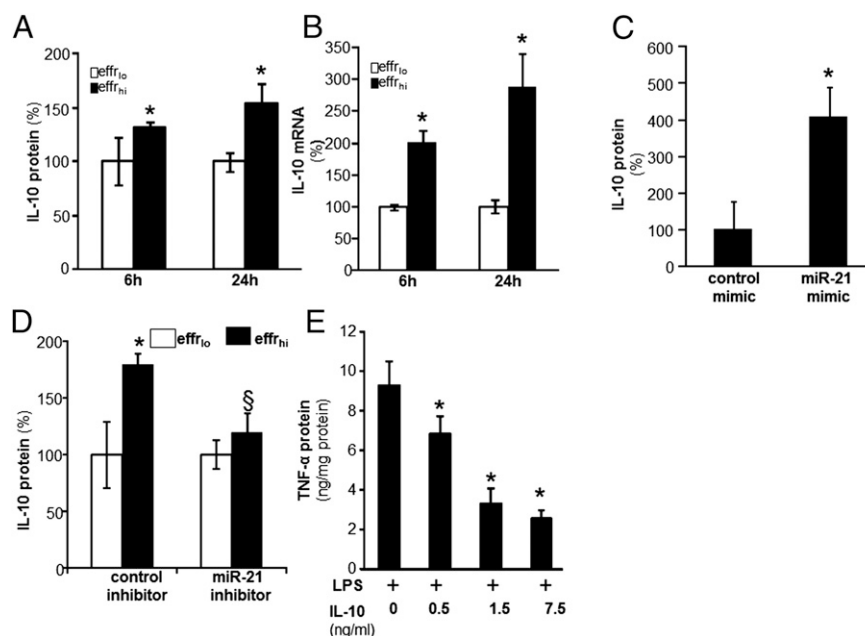


**FIGURE 7.** Successful efferocytosis potentiates inducible IL-10 expression via a miR-21-dependent mechanism. **(A and B)** For efferocytosis assay, blood MDMs were cocultured with either viable (effr<sub>1o</sub>) or apoptotic (effr<sub>ni</sub>) Jurkat T cells for 1 h. Nonefferocytosed cells were removed by washing with saline. Cells were treated with LPS (1  $\mu$ g/ml) for 6 and 24 h post efferocytosis. IL-10 **(A)** protein and **(B)** mRNA expression was measured using ELISA and quantitative PCR, respectively. Data are mean  $\pm$  SD ( $n = 4$ ); \* $p < 0.05$  compared with macrophages cultured with the effr<sub>1o</sub> group. **(C)** MDMs were transfected with miRIDIAN hsa-miR-21 mimic or control mimic to increase miR-21 levels. Cells were activated with LPS (1  $\mu$ g/ml) for 24 h after forced expression of miR-21 in MDMs. The IL-10 protein levels in cells were determined using ELISA. Data are mean  $\pm$  SD ( $n = 4$ ); \* $p < 0.05$  compared with macrophages transfected with control mimic. **(D)** MDMs were transfected with miRIDIAN hsa-miR-21 hairpin single-stranded inhibitor or control inhibitor to knock down miR-21 levels. Cells were subjected to efferocytosis followed by activation with LPS (1  $\mu$ g/ml) for 24 h after knockdown of miR-21 in MDMs. The IL-10 protein levels in cells were determined using ELISA. Data are mean  $\pm$  SD ( $n = 3$ ); \* $p < 0.05$  compared with macrophages cultured with the effr<sub>1o</sub> group, \* $p < 0.05$  compared with macrophages transfected with control inhibitor. **(E)** MDMs were treated with recombinant human IL-10 for 1 h followed by LPS (1  $\mu$ g/ml) activation for 24 h. The TNF- $\alpha$  protein levels in cells were determined using ELISA. Data are mean  $\pm$  SD ( $n = 4$ ); \* $p < 0.05$  compared with macrophages untreated with IL-10.

for a direct role of PDCD4 in LPS-induced IL-10 expression, knockdown of PDCD4 by siRNA was achieved (Fig. 8C). Such knockdown resulted in  $\sim 80\%$  lowering of PDCD4 protein levels (Fig. 8C) and augmented LPS-induced IL-10 expression response (Fig. 8D, 8E). These data establish that PDCD4 is directly implicated in LPS-induced IL-10 expression.

Pharmacological inhibition of JNK (420119 JNK Inhibitor II) significantly inhibited LPS-induced IL-10 protein expression, indicating the involvement of JNK in IL-10 expression (Fig. 9A). Knockdown of cellular c-Jun using siRNA (Fig. 9C,  $\sim 75\%$   $\downarrow$ c-Jun) also resulted in significant downregulation of inducible IL-10 protein expression, demonstrating a direct role of c-Jun and JNK in LPS-induced IL-10 expression in human MDMs (Fig. 9B). Efferocytosis or delivery of miR-21 mimic to cells induced the transcriptional activity of AP-1 (Fig. 9D, 9E). Likewise, knockdown of PDCD4 increased phospho-c-Jun levels (Fig. 9F), establishing that efferocytosis, miR-21, and PDCD4 can regulate the c-Jun-AP-1 pathway, which in turn controls inducible IL-10 expression (Fig. 10).

## Discussion

At the injury site, efficient dead cell clearance, or efferocytosis, is a prerequisite for the timely resolution of inflammation (4–7). Successful engulfment of apoptotic cells by activated macrophages triggers potent anti-inflammatory and immunosuppressive mechanisms. Following efferocytosis, wound-associated activated macrophages produce anti-inflammatory cytokines such as IL-10 and suppress the release of proinflammatory mediators, including TNF- $\alpha$  (41, 49, 50). The current study recognizes miR-21 as being

directly implicated in switching wound-associated macrophages to an anti-inflammatory mode following successful engulfment of apoptotic cells at the site of injury.

LPS engagement of TLR4 is known to initiate a cascade of signaling events that culminate in the production of inflammatory cytokines by macrophages. Recent studies suggest that negative regulatory control mechanisms exist to limit the toxic effects of LPS (48). Identified as one of the first mammalian miRs, the miR-21 sequence is strongly conserved throughout evolution (24). miR-21, initially described as “oncomir,” is known to be a common inflammation-inducible miR (19, 20, 24). Suggestive evidence supports the idea that LPS-induced miR-21 expression serves as a negative regulatory mechanism to curb the deleterious effects of LPS (48). The current study demonstrates that potentiation of LPS-induced miR-21 expression following efferocytosis may function as an effective anti-inflammatory response that limits LPS-induced inflammation.

PTEN is validated as a target gene for miR-21 (22, 51). The role of PTEN in infection and inflammation has been addressed (52–54). Of note in the context of this study is the observation that PTEN facilitates LPS-induced TNF- $\alpha$  production. In PTEN<sup>-/-</sup> macrophages, LPS-induced TNF- $\alpha$  production was blunted (53, 54). PTEN is a dual protein-lipid phosphatase that dephosphorylates the secondary messenger produced by PI3K and interrupts the downstream activation of Akt (55–57). Thus, downregulation of PTEN activity favors sustained activation of the PI3K/Akt pathway. Activated Akt phosphorylates and inhibits the activity of GSK3 $\beta$ , a substrate for Akt (58). Phosphorylation of GSK3 $\beta$  by Akt at the N-terminal region serine 9 renders GSK3 $\beta$  inactive

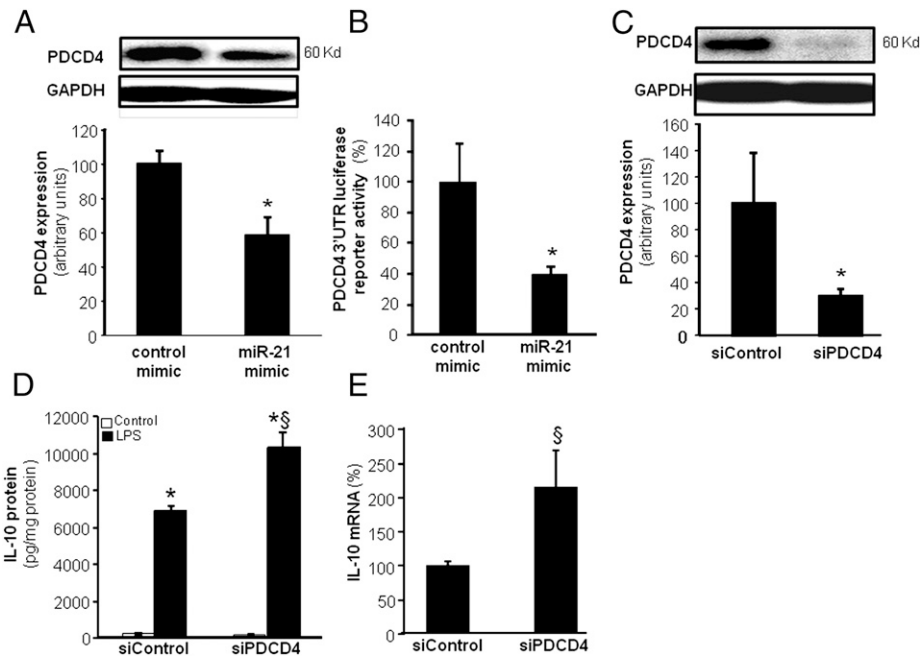


**FIGURE 8.** MiR-21 regulates IL-10 expression via PDCD4. **(A)** PDCD4 expression in MDMs transfected with miRIDIAN hsa-miR-21 mimic or control mimic. PDCD4 levels were determined using Western blot. Quantification of PDCD4 level was performed using densitometry, and the data were normalized to  $\beta$ -actin. Data are mean  $\pm$  SD ( $n = 3$ ); \* $p < 0.05$  compared with control mimic transfected cells. **(B)** To demonstrate that PDCD4 is a direct target for miR-21, HEK 293 cells were infected with lenti Luc-PDCD4-3'UTR plasmid along with either miR-21 mimic or control mimic. Data represent mean  $\pm$  SD ( $n = 4$ ); \* $p < 0.05$  compared with control transfected cells. **(C)** PDCD4 protein expression was measured using Western blot in MDMs transfected with siPDCD4 (100 nM) or siControl. Quantification of PDCD4 level was performed using densitometry. Data are mean  $\pm$  SD ( $n = 3$ ); \* $p < 0.05$  compared with siControl-transfected cells. **(D and E)** MDMs were transfected with siPDCD4 or siControl. Cells were activated with LPS (1  $\mu$ g/ml) for 24 h after knockdown of PDCD4 in MDMs. **(D)** IL-10 protein and **(E)** IL-10 mRNA were determined using ELISA and quantitative PCR, respectively. Data are mean  $\pm$  SD ( $n = 4$ ); \* $p < 0.05$  compared with non-LPS-treated cells, § $p < 0.05$  compared with siControl LPS-treated group.

(46). This work demonstrates that efferocytosis-induced miR-21, by silencing PTEN and GSK3 $\beta$ , tempers the LPS-induced inflammatory response.

Following successful efferocytosis, inhibition of NF- $\kappa$ B leads to anti-inflammatory responses, such as downregulation of inducible TNF- $\alpha$  production (8). Ubiquitously expressed, the NF- $\kappa$ B family of transcription factors regulates the expression of numerous genes implicated in immunity and inflammation (59). Vertebrate Rel/NF- $\kappa$ B transcription factors include RelA, RelB, c-Rel, p50/p105, and p52/p100 (59). NF- $\kappa$ B resides in the cytoplasm of cells in an inactive form bound to the inhibitor I $\kappa$ B. Activation of NF- $\kappa$ B is initiated through phosphorylation of I $\kappa$ B $\alpha$  by a macromolecular cytoplasmic IKK complex (59). Once activated, NF- $\kappa$ B is released from I $\kappa$ B and translocates to the nucleus, where it can drive gene expression, such as that of TNF- $\alpha$  (42). Inducible activation of NF- $\kappa$ B is further controlled by posttranslational modifications such as phosphorylation of the NF- $\kappa$ B subunit p65 as well as interaction with transcriptional coactivators (43). Multiple controls in the regulation of NF- $\kappa$ B activity suggest a complex and microenvironment-dependent function for this transcription factor. It has been proposed that GSK3 $\beta$  is a point of convergence of many signaling pathways, including that of the NF- $\kappa$ B signaling pathway (60). GSK3 $\beta$  inhibits NF- $\kappa$ B activity by lowering DNA binding (60). This work demonstrates that miR-21 controls NF- $\kappa$ B activation via silencing of GSK3 $\beta$ . This observation unveils a novel pathway wherein miR-21 blunts LPS-induced NF- $\kappa$ B activation by silencing PTEN and GSK3 $\beta$ .

Efferocytosis triggers release of anti-inflammatory cytokine IL-10 in macrophages (49). IL-10 is among the most prominent anti-inflammatory cytokines released following inflammation (61). The

idea that IL-10 acts as an anti-inflammatory molecule originated from studies showing blunted production of a large spectrum of proinflammatory cytokines by cells of monocytic lineage (47, 61). Although a number of studies described the release of IL-10 following efferocytosis (7, 41, 62), underlying mechanisms remain obscure. In this work, stimulation of TLR4 by LPS after efferocytosis resulted in increased abundance of miR-21, which in turn silenced PDCD4 (programmed cell death 4) and elevated IL-10 protein levels. These findings indicated that the miR-21-PDCD4 pathway may be involved in efferocytosis-induced anti-inflammatory IL-10 production in macrophages. Initially identified as a protein the abundance of which was increased by apoptotic stimuli and later characterized as a tumor suppressor, PDCD4 regulates both tumorigenesis and inflammation (63). The suppressive effect of PDCD4 on LPS-induced IL-10 expression was suggested to occur at the translational level (48). In the current study, knockdown of PDCD4 up-regulated IL-10 mRNA. This observation prompted us to look for miR-21 and PDCD4 dependent transcriptional control of IL-10. PDCD4 is known to block c-Jun activation by inhibiting the expression of MAP4K1 (MAPK kinase kinase 1; also known as hematopoietic progenitor kinase 1), a kinase upstream of JNK (64). Jun/AP-1 proteins are known to be involved in transcriptional activation of IL-10 in monocytic cells (65). Results of this work demonstrate that the miR-21-PDCD4 pathway favors c-Jun expression and AP-1 transactivation. Furthermore, it is established that c-Jun plays a critical role in supporting inducible IL-10 expression. Taken together, these observations demonstrate that following efferocytosis, miR-21 induction in macrophages silences PDCD4, therefore favoring Jun-AP-1 activity, resulting in higher production of anti-inflammatory IL-10.

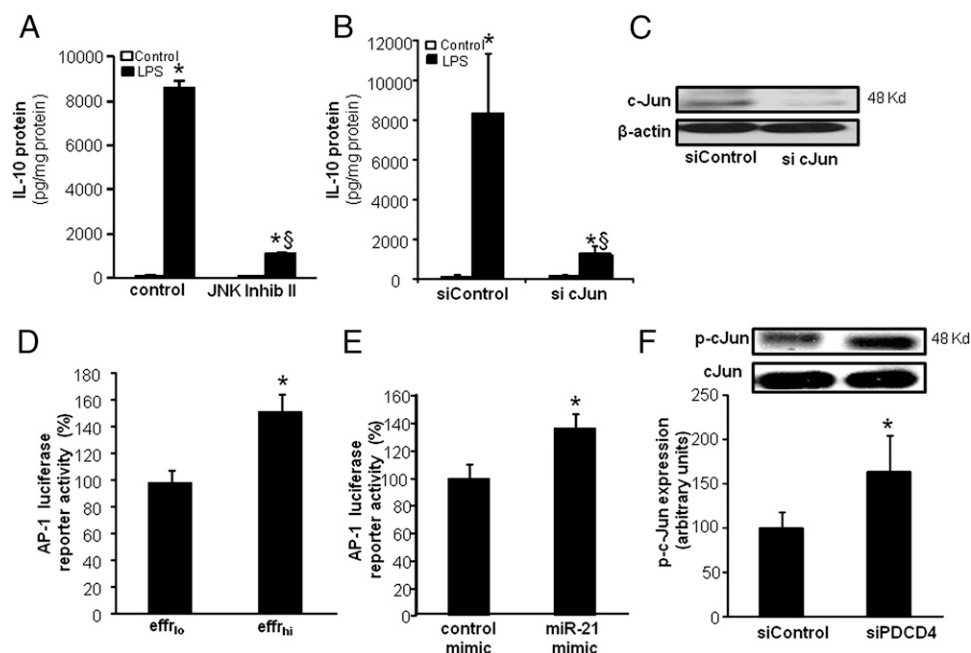


**FIGURE 9.** MiR-21 potentiated inducible IL-10 expression via a PDCD4-c-Jun-AP-1 pathway. **(A)** IL-10 protein expression was measured in MDMs treated with 20  $\mu$ M JNK inhibitor II, followed by LPS treatment. Data are mean  $\pm$  SD ( $n = 4$ ). \* $p < 0.05$  compared with non-LPS-treated cells,  $^{\S}p < 0.05$  compared with control LPS-treated group. **(B)** MDMs were transfected with siControl or si cJun. Cells were activated with LPS (1  $\mu$ g/ml) for 24 h after knockdown of c-Jun in MDMs. IL-10 protein was determined using ELISA. Data are mean  $\pm$  SD ( $n = 4$ ); \* $p < 0.05$  compared with macrophages transfected with non-LPS treated cells,  $^{\S}p < 0.05$  compared with siControl LPS-treated group. **(C)** Representative image of c-Jun protein expression in MDMs transfected with siControl (100 nM) or si cJun. **(D)** AP-1 transcription activity in MDMs transiently transfected with AP-1-dependent luciferase reporter gene (Ad-AP-1-Luc) followed by coculture with either viable (effr<sub>10</sub>) or apoptotic (effr<sub>hi</sub>) Jurkat T cells for 1 h and LPS treatment for 24 h. Data represent mean  $\pm$  SD ( $n = 3$ ); \* $p < 0.05$  compared with effr<sub>10</sub> group. **(E)** HEK293 TLR4/IL-1R1/MD-2 cells were cotransfected with a pAP-1 luciferase and pRL-TK Renilla luciferase plasmids along with either miR-21 mimic or control mimic followed by LPS stimulation. Data represent mean  $\pm$  SD ( $n = 3$ ); \* $p < 0.05$  compared with control mimic transfected cells. **(F)** Phosphorylation of c-Jun (serine 73) in MDMs transfected with siPDCD4 or siControl followed by activation with LPS. Data are mean  $\pm$  SD ( $n = 3$ ). \* $p < 0.05$  compared with macrophages transfected with siControl.

The current work recognizes a regulatory loop wherein efferocytosis induces miR-21, which in turn promotes efferocytosis.

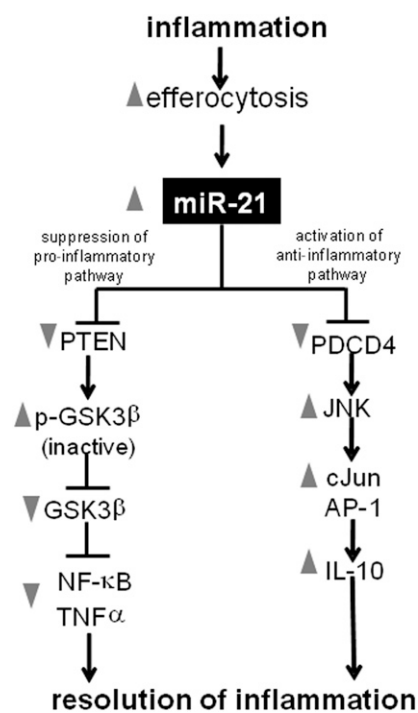


**FIGURE 10.** Central role of miR-21 in efferocytosis-dependent resolution of wound inflammation. miR-21 downregulates proinflammatory response via blocking the TNF- $\alpha$ -NF- $\kappa$ B pathway, and upregulates anti-inflammatory IL-10 via the AP-1 pathway.

Delivery of miR-21 to MDMs bolstered efferocytosis. This observation is consistent with the report that PTEN, a direct target of miR-21, downregulates engulfment of apoptotic cells (52). Furthermore, inducible TNF- $\alpha$ , known to inhibit efferocytosis (66), is repressed by miR-21. In conclusion, this work provides the first evidence, to our knowledge, directly implicating miRNA in the process of turning on an anti-inflammatory phenotype in the post-efferocytotic macrophage. Specifically, miR-21 is recognized as efferocytosis inducible in macrophages. Elevated macrophage miR-21 promotes efferocytosis and silences target genes such as PTEN and PDCD4, which in turn accounts for a net anti-inflammatory phenotype. Findings of this study underscore the significance of miRs in the resolution of inflammation.

## Disclosures

The authors have no financial conflicts of interest.

## References

- deCathelineau, A. M., and P. M. Henson. 2003. The final step in programmed cell death: phagocytes carry apoptotic cells to the grave. *Essays Biochem.* 39: 105–117.
- Gardai, S. J., D. L. Bratton, C. A. O'Gden, and P. M. Henson. 2006. Recognition ligands on apoptotic cells: a perspective. *J. Leukoc. Biol.* 79: 896–903.
- Vandivier, R. W., P. M. Henson, and I. S. Douglas. 2006. Burying the dead: the impact of failed apoptotic cell removal (efferocytosis) on chronic inflammatory lung disease. *Chest* 129: 1673–1682.
- Khanna, S., S. Biswas, Y. Shang, E. Collard, A. Azad, C. Kauh, V. Bhaskar, G. M. Gordillo, C. K. Sen, and S. Roy. 2010. Macrophage dysfunction impairs resolution of inflammation in the wounds of diabetic mice. *PLoS ONE* 5: e9539.
- Manfredi, A. A., M. Iannaccone, F. D'Auria, and P. Rovere-Querini. 2002. The disposal of dying cells in living tissues. *Apoptosis* 7: 153–161.
- Savill, J., I. Dransfield, C. Gregory, and C. Haslett. 2002. A blast from the past: clearance of apoptotic cells regulates immune responses. *Nat. Rev. Immunol.* 2: 965–975.
- Savill, J., and V. Fadok. 2000. Corpse clearance defines the meaning of cell death. *Nature* 407: 784–788.

8. Tibrewal, N., Y. Wu, V. D'mello, R. Akakura, T. C. George, B. Varnum, and R. B. Birge. 2008. Autophosphorylation docking site Tyr-867 in Mer receptor tyrosine kinase allows for dissociation of multiple signaling pathways for phagocytosis of apoptotic cells and down-modulation of lipopolysaccharide-inducible NF-kappaB transcriptional activation. *J. Biol. Chem.* 283: 3618–3627.
9. Ravichandran, K. S., and U. Lorenz. 2007. Engulfment of apoptotic cells: signals for a good meal. *Nat. Rev. Immunol.* 7: 964–974.
10. Henson, P. M. 2005. Dampening inflammation. *Nat. Immunol.* 6: 1179–1181.
11. Sen, C. K. 2011. MicroRNAs as new maestro conducting the expanding symphony orchestra of regenerative and reparative medicine. *Physiol. Genomics* 43: 517–520.
12. Sen, C. K., G. M. Gordillo, S. Khanna, and S. Roy. 2009. Micromanaging vascular biology: tiny microRNAs play big band. *J. Vasc. Res.* 46: 527–540.
13. Taganov, K. D., M. P. Boldin, K. J. Chang, and D. Baltimore. 2006. NF-kappaB-dependent induction of microRNA miR-146, an inhibitor targeted to signaling proteins of innate immune responses. *Proc. Natl. Acad. Sci. USA* 103: 12481–12486.
14. Asirvatham, A. J., W. J. Magner, and T. B. Tomasi. 2009. miRNA regulation of cytokine genes. *Cytokine* 45: 58–69.
15. Tili, E., C. M. Croce, and J. J. Michaille. 2009. miR-155: on the crosstalk between inflammation and cancer. *Int. Rev. Immunol.* 28: 264–284.
16. Sorrentino, A., C. G. Liu, A. Addario, C. Peschio, G. Scambia, and C. Ferlini. 2008. Role of microRNAs in drug-resistant ovarian cancer cells. *Gynecol. Oncol.* 111: 478–486.
17. Okada, H., G. Kohanbash, and M. T. Lotze. 2010. MicroRNAs in immune regulation—opportunities for cancer immunotherapy. *Int. J. Biochem. Cell Biol.* 42: 1256–1261.
18. Jiang, S., H. W. Zhang, M. H. Lu, X. H. He, Y. Li, H. Gu, M. F. Liu, and E. D. Wang. 2010. MicroRNA-155 functions as an Onco-miR in breast cancer by targeting the suppressor of cytokine signaling 1 gene. *Cancer Res.* 70: 3119–3127.
19. Roy, S., and C. K. Sen. 2011. MiRNA in innate immune responses: novel players in wound inflammation. *Physiol. Genomics* 43: 557–565.
20. Roy, S., and C. K. Sen. 2012. miRNA in wound inflammation and angiogenesis. *Microcirculation* 19: 224–232.
21. Fujita, S., T. Ito, T. Mizutani, S. Minoguchi, N. Yamamichi, K. Sakurai, and H. Iba. 2008. miR-21 Gene expression triggered by AP-1 is sustained through a double-negative feedback mechanism. *J. Mol. Biol.* 378: 492–504.
22. Roy, S., S. Khanna, S. R. Hussain, S. Biswas, A. Azad, C. Rink, S. Gnyawali, S. Shilo, G. J. Nuovo, and C. K. Sen. 2009. MicroRNA expression in response to murine myocardial infarction: miR-21 regulates fibroblast metalloproteinase-2 via phosphatase and tensin homologue. *Cardiovasc. Res.* 82: 21–29.
23. Meng, F., R. Henson, M. Lang, H. Wehbe, S. Maheshwari, J. T. Mendell, J. Jiang, T. D. Schmittgen, and T. Patel. 2006. Involvement of human microRNA in growth and response to chemotherapy in human cholangiocarcinoma cell lines. *Gastroenterology* 130: 2113–2129.
24. Sen, C. K., and S. Roy. 2012. MicroRNA 21 in tissue injury and inflammation. *Cardiovasc. Res.* 96: 230–233.
25. Lu, T. X., A. Munitz, and M. E. Rothenberg. 2009. MicroRNA-21 is up-regulated in allergic airway inflammation and regulates IL-12p35 expression. *J. Immunol.* 182: 4994–5002.
26. Case, S. R., R. J. Martin, D. Jiang, M. N. Minor, and H. W. Chu. 2011. MicroRNA-21 inhibits toll-like receptor 2 agonist-induced lung inflammation in mice. *Exp. Lung Res.* 37: 500–508.
27. Recchiuti, A., S. Krishnamoorthy, G. Fredman, N. Chiang, and C. N. Serhan. 2011. MicroRNAs in resolution of acute inflammation: identification of novel resolvins D1-miRNA circuits. *FASEB J.* 25: 544–560.
28. Günzl, P., and G. Schabbauer. 2008. Recent advances in the genetic analysis of PTEN and PI3K innate immune properties. *Immunobiology* 213: 759–765.
29. Ganesh, K., A. Das, R. Dickerson, S. Khanna, N. L. Parinandi, G. M. Gordillo, C. K. Sen, and S. Roy. 2012. Prostaglandin E<sub>2</sub> induces oncostatin M expression in human chronic wound macrophages through Axl receptor tyrosine kinase pathway. *J. Immunol.* 189: 2563–2573.
30. Roy, S., S. Khanna, C. Rink, S. Biswas, and C. K. Sen. 2008. Characterization of the acute temporal changes in excisional murine cutaneous wound inflammation by screening of the wound-edge transcriptome. *Physiol. Genomics* 34: 162–184.
31. Roy, S., S. Khanna, T. Rink, J. Radtke, W. T. Williams, S. Biswas, R. Schnitt, A. R. Strauch, and C. K. Sen. 2007. P21/waf1/cip1/sd1 as a central regulator of inducible smooth muscle actin expression and differentiation of cardiac fibroblasts to myofibroblasts. *Mol. Biol. Cell* 18: 4837–4846.
32. Chan, Y. C., S. Khanna, S. Roy, and C. K. Sen. 2011. miR-200b targets Ets-1 and is down-regulated by hypoxia to induce angiogenic response of endothelial cells. *J. Biol. Chem.* 286: 2047–2056.
33. Chan, Y. C., S. Roy, Y. Huang, S. Khanna, and C. K. Sen. 2012. The microRNA miR-199a-5p down-regulation switches on wound angiogenesis by de-repressing the v-ets erythroblastosis virus E26 oncogene homolog 1-matrix metalloproteinase-1 pathway. *J. Biol. Chem.* 287: 41032–41043.
34. Roy, S., S. Khanna, A. A. Bickerstaff, S. V. Subramanian, M. Atalay, M. Bierl, S. Pendyala, D. Levy, N. Sharma, M. Venojarvi, et al. 2003. Oxygen sensing by primary cardiac fibroblasts: a key role of p21(Waf1/Cip1/Sd1). *Circ. Res.* 92: 264–271.
35. Roy, S., S. Khanna, K. Nallu, T. K. Hunt, and C. K. Sen. 2006. Dermal wound healing is subject to redox control. *Mol. Ther.* 13: 211–220.
36. Biswas, S., S. Roy, J. Banerjee, S. R. Hussain, S. Khanna, G. Meenakshisundaram, P. Kuppusamy, A. Friedman, and C. K. Sen. 2010. Hypoxia inducible microRNA 210 attenuates keratinocyte proliferation and impairs closure in a murine model of ischemic wounds. *Proc. Natl. Acad. Sci. USA* 107: 6976–6981.
37. Seshadri, S., Y. Kannan, S. Mitra, J. Parker-Barnes, and M. D. Wewers. 2009. MAIL regulates human monocyte IL-6 production. *J. Immunol.* 183: 5358–5368.
38. Wan, E., X. Y. Yeap, S. Dehn, R. L. Terry, M. L. Novak, S. Zhang, S. Iwata, X. Han, S. Homma, K. Drosatos, et al. 2013. Enhanced efferocytosis of apoptotic cardiomyocytes through MER tyrosine kinase links acute inflammation resolution to cardiac repair after infarction. *Circ. Res.* 113: 1004–1012.
39. Erwig, L. P., and P. M. Henson. 2007. Clearance of apoptotic cells by phagocytes. *Cell Death Differ.* 15: 243–250.
40. Fadok, V. A. 1999. Clearance: the last and often forgotten stage of apoptosis. *J. Mammary Gland Biol. Neoplasia* 4: 203–211.
41. Fadok, V. A., D. L. Bratton, A. Konowal, P. W. Freed, J. Y. Westcott, and P. M. Henson. 1998. Macrophages that have ingested apoptotic cells in vitro inhibit proinflammatory cytokine production through autocrine/paracrine mechanisms involving TGF-beta, PGE2, and PAF. *J. Clin. Invest.* 101: 890–898.
42. Collart, M. A., P. Baeuerle, and P. Vassalli. 1990. Regulation of tumor necrosis factor alpha transcription in macrophages: involvement of four kappa B-like motifs and of constitutive and inducible forms of NF-kappa B. *Mol. Cell. Biol.* 10: 1498–1506.
43. Yang, F., E. Tang, K. Guan, and C. Y. Wang. 2003. IKK beta plays an essential role in the phosphorylation of RelA/p65 on serine 536 induced by lipopolysaccharide. *J. Immunol.* 170: 5630–5635.
44. Schmid, A. C., R. D. Byrne, R. Vilar, and R. Woscholski. 2004. Bisperoxovanadium compounds are potent PTEN inhibitors. *FEBS Lett.* 566: 35–38.
45. Stambolic, V., A. Suzuki, J. L. de la Pompa, G. M. Brothers, C. Mirtsos, T. Sasaki, J. Ruland, J. M. Penninger, D. P. Siderovski, and T. W. Mak. 1998. Negative regulation of PKB/Akt-dependent cell survival by the tumor suppressor PTEN. *Cell* 95: 29–39.
46. Sutherland, C., I. A. Leighton, and P. Cohen. 1993. Inactivation of glycogen synthase kinase-3 beta by phosphorylation: new kinase connections in insulin and growth-factor signalling. *Biochem. J.* 296: 15–19.
47. de Waal Malefyt, R., J. Abrams, B. Bennett, C. G. Figdor, and J. E. de Vries. 1991. Interleukin 10(IL-10) inhibits cytokine synthesis by human monocytes: an autoregulatory role of IL-10 produced by monocytes. *J. Exp. Med.* 174: 1209–1220.
48. Sheedy, F. J., E. Palsson-McDermott, E. J. Hennessy, C. Martin, J. J. O'Leary, Q. Ruan, D. S. Johnson, Y. Chen, and L. A. O'Neill. 2010. Negative regulation of TLR4 via targeting of the proinflammatory tumor suppressor PDCD4 by the microRNA miR-21. *Nat. Immunol.* 11: 141–147.
49. Voll, R. E., M. Herrmann, E. A. Roth, C. Stach, J. R. Kalden, and I. Girkontaite. 1997. Immunosuppressive effects of apoptotic cells. *Nature* 390: 350–351.
50. Huynh, M. L., V. A. Fadok, and P. M. Henson. 2002. Phosphatidylserine-dependent ingestion of apoptotic cells promotes TGF-beta1 secretion and the resolution of inflammation. *J. Clin. Invest.* 109: 41–50.
51. Meng, F., R. Henson, H. Wehbe-Janeck, K. Ghoshal, S. T. Jacob, and T. Patel. 2007. MicroRNA-21 regulates expression of the PTEN tumor suppressor gene in human hepatocellular cancer. *Gastroenterology* 133: 647–658.
52. Mondal, S., S. Ghosh-Roy, F. Loison, Y. Li, Y. Jia, C. Harris, D. A. Williams, and H. R. Luo. 2011. PTEN negatively regulates engulfment of apoptotic cells by modulating activation of Rac GTPase. *J. Immunol.* 187: 5783–5794.
53. Cao, X., G. Wei, H. Fang, J. Guo, M. Weinstein, C. B. Marsh, M. C. Ostrowski, and S. Tridandapani. 2004. The inositol 3-phosphatase PTEN negatively regulates Fc gamma receptor signaling, but supports Toll-like receptor 4 signaling in murine peritoneal macrophages. *J. Immunol.* 172: 4851–4857.
54. Günzl, P., K. Bauer, E. Hainzl, U. Matt, B. Dillinger, B. Mahr, S. Knapp, B. R. Binder, and G. Schabbauer. 2010. Anti-inflammatory properties of the PI3K pathway are mediated by IL-10/DUSP regulation. *J. Leukoc. Biol.* 88: 1259–1269.
55. Rosivatz, E. 2007. Inhibiting PTEN. *Biochem. Soc. Trans.* 35: 257–259.
56. Maehama, T., and J. E. Dixon. 1999. PTEN: a tumour suppressor that functions as a phospholipid phosphatase. *Trends Cell Biol.* 9: 125–128.
57. Georgescu, M. M. 2010. PTEN tumor suppressor network in PI3K-Akt pathway control. *Genes Cancer* 1: 1170–1177.
58. Cross, D. A., D. R. Alessi, P. Cohen, M. Andjelkovich, and B. A. Hemmings. 1995. Inhibition of glycogen synthase kinase-3 by insulin mediated by protein kinase B. *Nature* 378: 785–789.
59. Ghosh, S., M. J. May, and E. B. Kopp. 1998. NF-kappa B and Rel proteins: evolutionarily conserved mediators of immune responses. *Annu. Rev. Immunol.* 16: 225–260.
60. Steinbrecher, K. A., W. Wilson, III, P. C. Cogswell, and A. S. Baldwin. 2005. Glycogen synthase kinase 3beta functions to specify gene-specific, NF-kappaB-dependent transcription. *Mol. Cell. Biol.* 25: 8444–8455.
61. Pretolani, M. 1999. Interleukin-10: an anti-inflammatory cytokine with therapeutic potential. *Clin. Exp. Allergy* 29: 1164–1171.
62. McDonald, P. P., V. A. Fadok, D. Bratton, and P. M. Henson. 1999. Transcriptional and translational regulation of inflammatory mediator production by endogenous TGF-beta in macrophages that have ingested apoptotic cells. *J. Immunol.* 163: 6164–6172.
63. Merline, R., K. Moreth, J. Beckmann, M. V. Nastase, J. Zeng-Brouwers, J. G. Tralhão, P. Lemarchand, J. Pfeilschifter, R. M. Schaefer, R. V. Iozzo, and L. Schaefer. 2011. Signaling by the matrix proteoglycan decorin controls inflammation and cancer through PDCD4 and MicroRNA-21. *Sci. Signal.* 4: ra75.
64. Wang, Q., Y. Zhang, and H. S. Yang. 2012. Pdc4 knockdown up-regulates MAP4K1 expression and activation of AP-1 dependent transcription through c-Myc. *Biochim. Biophys. Acta* 1823: 1807–1814.
65. Wang, Z. Y., H. Sato, S. Kusam, S. Sehra, L. M. Toney, and A. L. Dent. 2005. Regulation of IL-10 gene expression in Th2 cells by Jun proteins. *J. Immunol.* 174: 2098–2105.
66. McPhillips, K., W. J. Janssen, M. Ghosh, A. Byrne, S. Gardai, L. Remigio, D. L. Bratton, J. L. Kang, and P. Henson. 2007. TNF-alpha inhibits macrophage clearance of apoptotic cells via cytosolic phospholipase A2 and oxidant-dependent mechanisms. *J. Immunol.* 178: 8117–8126.